

# Development of HF ocean radar in Japan

Yukiharu Hisaki

Department of Physics and Earth Sciences

University of the Ryukyus

Okinawa 903-0213, Japan

Telephone: +81-98-895-8515

Fax: +81-98-895-8552

Email: hisaki@sci.u-ryukyu.ac.jp

**Abstract**—The HF ocean radar was developed in Japan from 1987 by Okinawa Radio Observatory, Communications Research Laboratory. We measured ocean surface currents and developed the method to estimate wave spectra. The observations of ocean surface currents were conducted in various areas. The observation in the east of Okinawa, where mesoscale eddies are dominant, is presented. We can observe the convergent zone associated with the front of a mesoscale eddy. Furthermore, the short-wave directions and spread parameters were estimated from first-order scattering. We also developed the method to estimate ocean wave spectra from Doppler spectra. We extended the theory of HF radio wave scattering from the sea surface. It is possible to explain the underestimation of waveheights, which was previously pointed out.

## I. INTRODUCTION

HF ocean radar is used to measure ocean surface currents and waves by radiating high-frequency radio waves and analyzing backscattered signals from the ocean. This technique is based on the backscattering of radio waves by resonant surface waves of one half the incident radar wavelength. This is called Bragg scattering, and its Doppler frequency (Bragg frequency) is determined from the linear dispersion relationship of surface waves. However, in practice, the position of first-order scattering of the measured Doppler spectrum is somewhat different from the Bragg frequency. This difference is due to the advection of the surface waves by ocean currents. We can, therefore, estimate the radial component of the ocean current by estimating the frequency shift of the Bragg peaks. Furthermore, the two first-order Bragg peaks are surrounded by the second-order continuum, which is called second-order scattering. All of the wave components contribute to second-order scattering, and we can estimate ocean wave spectra from second-order scattering.

The development of HF ocean radar in Japan began from 1987 in Okinawa Radio Observatory (Okinawa Subtropical Environment Remote-Sensing Center), Communications Research Laboratory. Test observations were conducted only by one radar from 1989. We developed the second radar in 1991, and it is possible to measure ocean current vectors. We measured ocean surface currents and developed the method to estimate wave spectra. The objective of the report is to present past and present studies on HF radar oceanography in Japan. The topics are (1) measurement of ocean surface currents ([1]), (2) short-wave directional properties ([2]), (3) wave directional

Transmitter & receiver	
Center frequency	24.515 MHz
Transmitted power	100 W
Sweep bandwidth	100 kHz
Radar type	FMICW
Range resolution	1.5 km
Antenna	
Antenna type	10-element phased array antenna
Aperture length	54.9 m
Beamwidth	15°
Beam directions	0 ± 45° (13 directions)
Polarization	vertical

TABLE I  
CHARACTERISTICS OF THE HF OCEAN RADAR

spectrum estimation ([3]), and (4) HF radio wave scattering from the sea ([4], [5]).

## II. RADAR SYSTEM

Table 1 is the specification of HF radar system. The radio frequency is 24.5MHz and the FMICW (Frequency Modulated Interrupted Continuous Wave) radar is used. The phased array system is used, so the large area for the deployment is necessary. The spatial range resolution of the radar is 1.5km. The radar beam can be directed from  $-45^\circ$  to  $+45^\circ$  in  $7.5^\circ$  step. The beam direction is controlled by the hardware in real time. It takes 10 minutes to measured one direction, therefore, we repeated the measurements every 2 hours in the observation.

## III. OBSERVATION OF CURRENTS

### A. Comparison of currents

Figure 1 is the observation area by HF ocean radar. The radars are located at site A ( $26^\circ 7.19' N$ ,  $127^\circ 45.78' E$ ) and B ( $26^\circ 18.63' N$ ,  $127^\circ 50.25' E$ ). The region east of Okinawa is affected by mesoscale eddies. The HF radar observation was conducted from 15 April 1998 to 15 May 1998 in the east of Okinawa Island (around  $26^\circ N$ ,  $128^\circ E$ ). The current meter was deployed at the location P (Payao). The water depth of the deployment was 4 m. The wind station is at I (Itokazu) in Figure 1. The location of the wave measurement is at Ky (Kyan) in Figure 1.

We compared HF-ocean-radar-derived currents with in-situ current data [1]. Table II shows the summary of the comparison. The number of samples in the comparison was 309.

Report Documentation Page				Form Approved OMB No. 0704-0188	
Public reporting burden for the collection of information is estimated to average 1 hour per response, including the time for reviewing instructions, searching existing data sources, gathering and maintaining the data needed, and completing and reviewing the collection of information. Send comments regarding this burden estimate or any other aspect of this collection of information, including suggestions for reducing this burden, to Washington Headquarters Services, Directorate for Information Operations and Reports, 1215 Jefferson Davis Highway, Suite 1204, Arlington VA 22202-4302. Respondents should be aware that notwithstanding any other provision of law, no person shall be subject to a penalty for failing to comply with a collection of information if it does not display a currently valid OMB control number.					
1. REPORT DATE <b>14 APR 2005</b>		2. REPORT TYPE <b>N/A</b>		3. DATES COVERED <b>-</b>	
4. TITLE AND SUBTITLE <b>Development of HF ocean radar in Japan</b>				5a. CONTRACT NUMBER	
				5b. GRANT NUMBER	
				5c. PROGRAM ELEMENT NUMBER	
6. AUTHOR(S)				5d. PROJECT NUMBER	
				5e. TASK NUMBER	
				5f. WORK UNIT NUMBER	
7. PERFORMING ORGANIZATION NAME(S) AND ADDRESS(ES) <b>Department of Physics and Earth Sciences University of the Ryukyus Okinawa 9030213, Japan</b>				8. PERFORMING ORGANIZATION REPORT NUMBER	
9. SPONSORING/MONITORING AGENCY NAME(S) AND ADDRESS(ES)				10. SPONSOR/MONITOR'S ACRONYM(S)	
				11. SPONSOR/MONITOR'S REPORT NUMBER(S)	
12. DISTRIBUTION/AVAILABILITY STATEMENT <b>Approved for public release, distribution unlimited</b>					
13. SUPPLEMENTARY NOTES <b>See also ADM001798, Proceedings of the International Conference on Radar (RADAR 2003) Held in Adelaide, Australia on 3-5 September 2003.</b>					
14. ABSTRACT					
15. SUBJECT TERMS					
16. SECURITY CLASSIFICATION OF:			17. LIMITATION OF ABSTRACT <b>UU</b>	18. NUMBER OF PAGES <b>5</b>	19a. NAME OF RESPONSIBLE PERSON
a. REPORT <b>unclassified</b>	b. ABSTRACT <b>unclassified</b>	c. THIS PAGE <b>unclassified</b>			

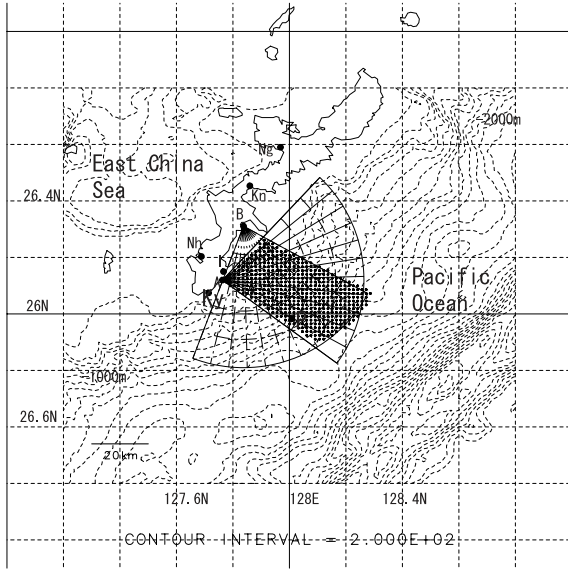


Fig. 1. Map of observation area

The correlations are greater than 0.85, and the root-mean-

	$u_P - u_r$	$v_P - v_r$
Correlation	0.87	0.89
rms difference ( $\text{cms}^{-1}$ )	11.68	10.47
Slope	1.015	1.047
Bias ( $\text{cms}^{-1}$ )	-3.89	0.043

TABLE II

COMPARISON BETWEEN HF OCEAN RADAR-DERIVED CURRENTS ( $u_r$ : EAST-WEST COMPONENT,  $v_r$ : NORTH-SOUTH COMPONENT) AND CURRENT METER-MEASURED CURRENTS AT PAYAO ( $u_P$ : EAST-WEST COMPONENT,  $v_P$ : NORTH-SOUTH COMPONENT).

square difference between the sensors is about  $11 \text{ cm s}^{-1}$ . The slopes and biases of the regression lines to the scatter plots are respectively about 1 and  $-4 \text{ cm s}^{-1}$ . From this comparison we conclude that radar-derived currents are sufficiently accurate for our purposes.

The HF radar-observation area appears to be affected by the mesoscale eddy front in the observation period from altimetric data and SST (sea surface temperature) data by TRMM (Tropical Rainfall Measuring Mission) microwave imager (Figure 2b). As indicated in Figures 2, prominent convergent zones were observed off Okinawa Island. For example, the southeastward and southwestward flows form a convergent zone in Figure 2a. The water depth of the convergent zone was greater than 1000 m. From NOAA/AVHRR imagery data, the

convergent zone was associate with a temperature front.

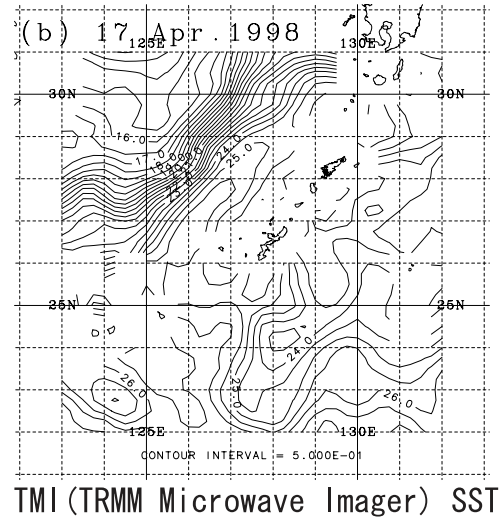
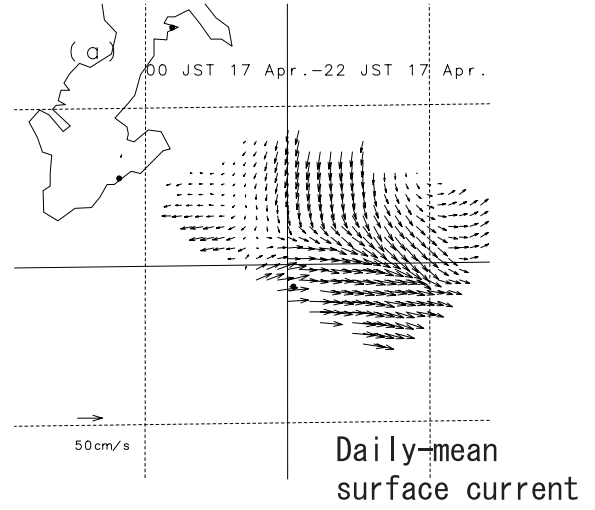


Fig. 2. (a) Daily mean currents, (b) daily SST data by TRMM microwave imager.

#### IV. SHORT-WAVE DIRECTION

We can estimate mean directions  $\theta_m$  and spread parameters  $s$  at the Bragg wavenumber. They are estimated from the ratio of first-order Doppler spectra. If the wave directional distribution is written as  $D(\theta) \propto \cos^{2s}(\theta/2)$ , where  $\theta$  is the wave direction relative to the mean direction, the first-order ratio is written as

$$R = \frac{D(\pi - \theta_m)}{D(-\theta_m)} = \tan^{2s}\left(\frac{\theta_m}{2}\right). \quad (1)$$

We can estimate  $\theta_m$  and  $s$  by two radars from (1). The short-wave direction is an indication of wind direction. We compared short-wave directions with wind directions. The comparison is shown in Figure 3. The agreement is good. The correlation was about 0.96, and the root-mean-square difference from the linear regression line was about  $31^\circ$ . The difference between

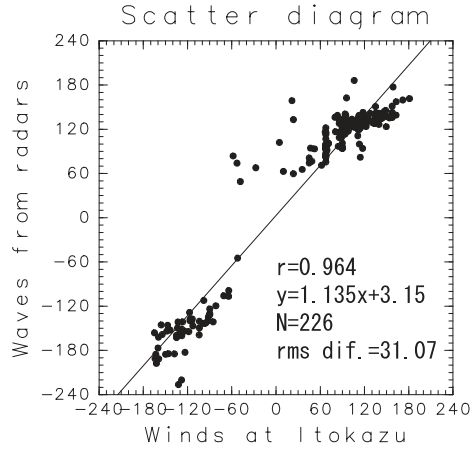


Fig. 3. Scatter diagram between wind directions with respect to the eastward direction (counterclockwise is positive) at Itokazu radar-estimated short-wave directions at the closest grid point to Itokazu.

wind directions (I in Figure 1) and radar-estimated short-wave directions are due to horizontal variations of winds and a time lag of short-wave response to a sudden wind shift. If the wind field is steady, the rms difference is small. For example, a previous study showed that the rms difference between the radar and buoy measurements was  $24^\circ$ , when high quality data were used [6].

Figure 4 shows radar-estimated short-wave directions in 25 April. The wind direction and short-wave directions were northeastward until 6 JST (Figure 4(a)). The short-wave directions in the northeastern part of HF ocean radar observation area were changed to southeastward (Figure 4(b)). We can see a discontinuity of short-wave directions in Figure 4(b). This is associate with a passage of an atmospheric front.

## V. WAVE SPECTRUM ESTIMATION

We developed the inversion method to estimate ocean wave spectra from second-order Doppler spectra [3]. The integral equation which relates Doppler spectra to the wave spectrum is discretized. Thus estimation of wave spectra is converted to the optimal problem. We demonstrated from the twin pair simulation that this method could estimate ocean wave directional spectra by two radars [3]. Figure 5 shows an example of wave spectrum estimation by dual radars. It is possible to estimate frequency spectra even if the Doppler spectrum is available in only a single direction. In this case, however, the solution

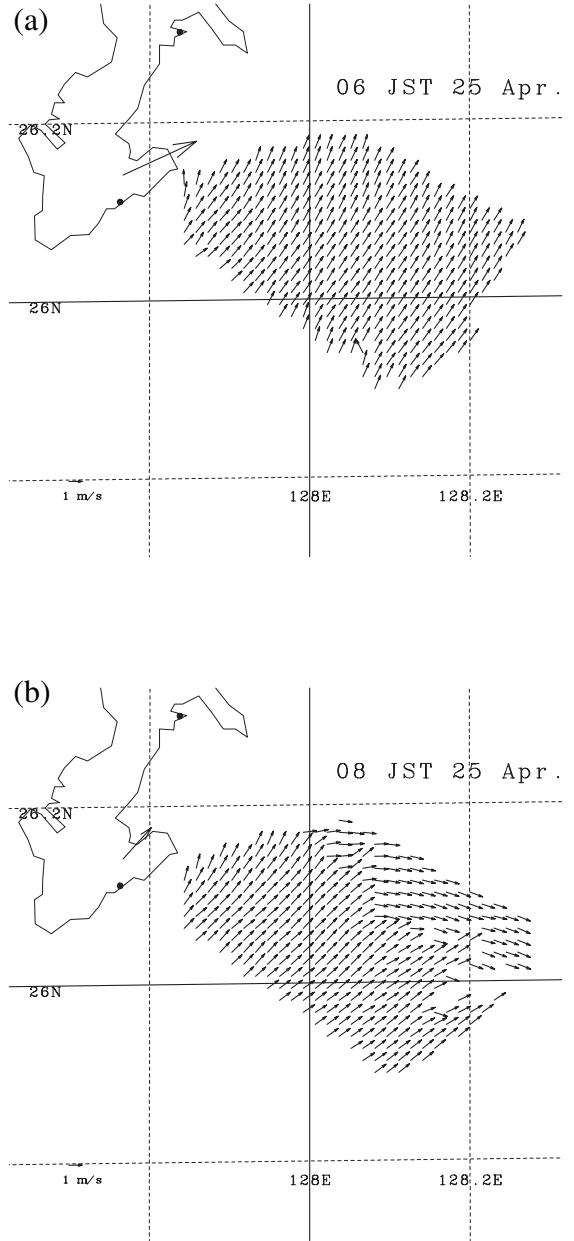
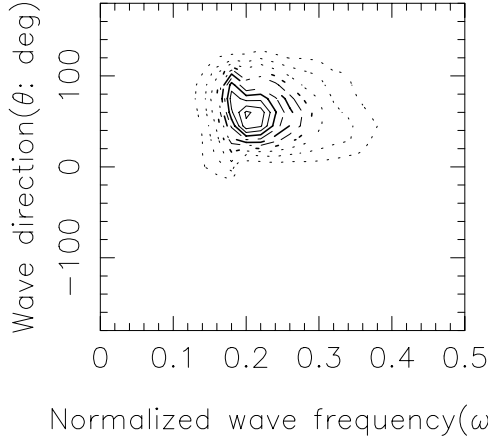


Fig. 4. Radar-estimated short-wave directions in 25 April 1998 and wind vector at Itokazu. (a) 6 JST, and (b) 8 JST.

of the directional spectrum tends to converge to a spectrum that is symmetrical to the beam direction. Even if the wave spectrum is dominant in a single direction, the solution may give two peaks in the wavenumber spectrum. One of them is the true peak and the other is the mirror image of it with respect to the beam direction. It is necessary to use two beam directions for estimation of wave directional spectra.

We compared buoy-measured with radar-estimated ocean wave spectra. The HF radar observation was conducted in the Japan sea from 5 to 20 March 1991, and the radar location was at Yura (near  $40^\circ\text{N}$ ,  $140^\circ$ ) [7]. We used only one radar, so we can only estimate frequency spectra. The frequency spectra

(a) Retrieved wave directional spectra



(b) True wave directional spectra

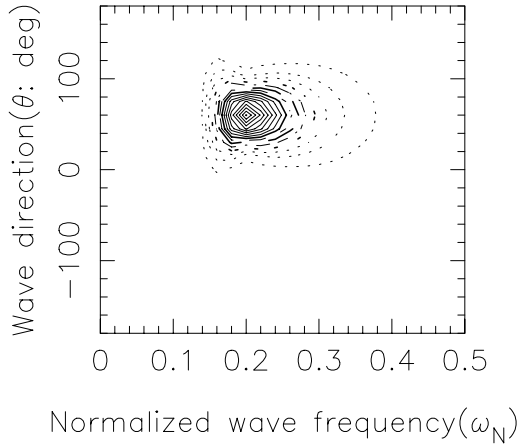


Fig. 5. Comparison of wave directional spectra as in the dual-beam case (crossing angle is  $90^\circ$ ). (a) Retrieved directional spectra, and (b) True directional spectra (thick dotted line= 2; thick dashed line= 3; thick solid line= 4; contour interval= 0.5).

were integrated and were converted to significant waveheights by calculating the square root of the integrated values and multiplying by the factor 4. Table III shows the summary of the comparison. The number of samples in the comparison was 173. The slope ( $a$ ) and bias ( $b$ ) of the regression line  $H_r = aH_b + b$ , where  $H_r$  and  $H_b$  are respectively radar-estimated and buoy-measured significant waveheights, were estimated. The correlation coefficients are more than 0.8 for total frequency band, and are large enough for practical use. However, there are bias errors resulting in overestimation of radar-estimated waveheight. The bias errors are primary created by external noise in Doppler spectra. The noise originates from natural (atmospheric) and man-made (environmental) sources. A method to reduce noise needs to be developed.

frequency band	Correlation	slope ( $a$ )	bias ( $b$ , m)
0.03–0.10 Hz	0.804	1.058	0.387
0.10–0.125 Hz	0.897	1.023	0.310
0.125–0.155 Hz	0.838	0.858	0.344
0.16–0.20 Hz	0.692	0.808	0.362
0.20–0.25 Hz	0.638	0.754	0.347
Total	0.858	0.948	0.718

TABLE III  
COMPARISON OF WAVE SPECTRA.

## VI. RADIO WAVE SCATTERING

The HF radio wave scattering theory, which is the basic equation to estimate ocean wave spectra, is derived from the second order perturbation method of electromagnetic field. However, we can expect that this theory does not apply in the case of high sea conditions. The radio frequency allocation is quite limited, and it is not feasible to use both high- and low-radio frequency according to the sea states. That is, it is not feasible for us to change radio frequencies according to the sea states. In the perturbation theory, the scattered electric field is written as  $E = E_1 + E_2 + E_3 + \dots$ , and the radar cross section is proportional to the power spectrum of the scattered electric field. If the first-order scattered field  $E_1$  is a Gaussian process with zero mean, the power is written as  $\langle |E|^2 \rangle_E = \langle |E_1|^2 + |E_2|^2 + E_1 E_3^* + E_1^* E_3 + \dots \rangle_E$ , where an asterisk denotes the complex conjugate and  $\langle \dots \rangle_E$  denotes the ensemble average. The term  $\langle |E_1|^2 \rangle_E$  corresponds to the first-order radar cross section and the term  $\langle |E_2|^2 \rangle_E$  corresponds to the second-order radar cross section. The terms  $\langle E_1 E_3^* \rangle_E$  (and  $\langle E_1^* E_3 \rangle_E$ ) are of the same order as the second-order radar cross section. These terms modify the first-order radar cross section, and they affect the estimation of waveheight, because the second-order radar cross section is normalized by first-order radar cross section. We calculated this correction term of first-order radar cross section [4]. Figure 6 is the result of the ratio of the correction term to the first-order radar cross section as a function of dominant wave frequency and direction. For example, 0.1 Hz of the dominant wave frequency corresponds to 4 m of the significant waveheight, the ratio is about 0.2. This means that if the correction is not considered, the waveheight is under-estimated by about 10 %. The under-estimation of waveheight is consistent with [8].

It is for higher-order correction of the first-order Bragg echoes, and it has no relation with the shape of second-order scatter scattering. If we see Doppler spectrum at high sea states, the shape of the Doppler spectra is different from predicted Doppler spectrum. In general, observed Doppler spectra are broaden at high sea states [7].

In order to explain this discrepancy between measured and predicted Doppler spectra, we calculated second-order Doppler spectra by considering the finite illuminated area [5]. Figure 7 is the result of the comparison. This is the VHF case and the radio frequency is 42 MHz. In these cases, the prediction appears to be improved. But there are still discrepancies as Figure 7a. This prediction should be improved further.

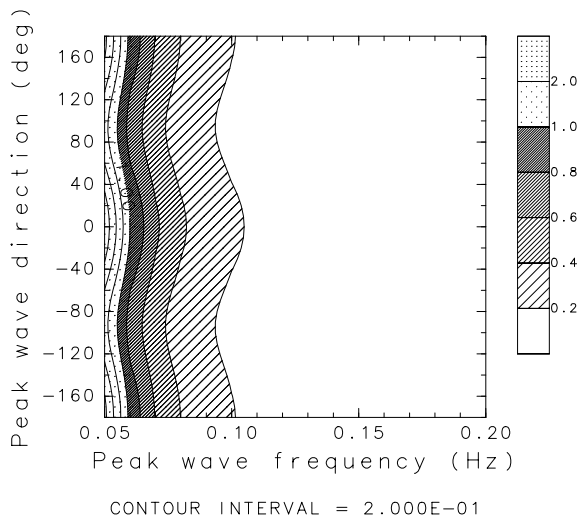


Fig. 6. Third-order correction term (corresponding to  $\langle E_1 E_3^* \rangle_E$  and  $\langle E_1^* E_3 \rangle_E$ ) relative to the first-order radar cross section as a function of peak wave frequencies and peak wave directions

## VII. SUMMARY

The report is summarized as follows:

(1) The agreement between measured and radar-estimated currents is good. (2) The convergent zone associated with mesoscale eddy is detected by HF ocean radar. (3) The agreement between wind directions and radar-estimated short-wave directions is good. (4) We developed the inversion method to estimate wave spectra. Comparisons with in-situ measurements are necessary further. (5) We extended the HF radio wave scattering theory, however, the further improvement of the theory to explain the broadening of second-order radar cross section is necessary.

## ACKNOWLEDGMENT

The authors would like to thank to staff of staff of Okinawa Radio Observatory (Okinawa Subtropical Environment Remote-Sensing Center), Communications Research Laboratory for providing Doppler spectrum data of HF ocean radars.

## REFERENCES

- [1] Y. Hisaki, T. Tokeshi, W. Fujiie, K. Sato, S. Fujii, "Surface current variability in east of Okinawa Island from remotely-sensed and in-situ observational data," *J. Geophys. Res.*, 106, 31057–31073, 2001.
- [2] Y. Hisaki, "Short-wave directional properties in the vicinity of atmospheric and oceanic fronts," *J. Geophys. Res.*, 107, doi:10.1029/2001JC000912, 2002.
- [3] Y. Hisaki, "Nonlinear inversion of the integral equation to estimate ocean wave spectra from HF radar," *Radio Sci.*, 31, 25–39, 1996.
- [4] Y. Hisaki, "Correction of amplitudes of Bragg lines in the sea echo Doppler spectrum of an ocean radar," *J. Atmos. and Oceanic Technol.*, 16, 1416–1433, 1999.
- [5] Y. Hisaki and M. Tokuda, "VHF and HF sea echo Doppler spectrum for a finite illuminated area," *Radio Sci.*, 36, 425–440, 2001.
- [6] J. A. Harlan and T. M. Georges An empirical relation between ocean-surface wind direction and the Bragg line ratio of HF radar sea echo spectra. *J Geophys Res.*, 99, 7971–7978, 1994.
- [7] Y. Hisaki and M. Tokuda, "Detection of nonlinear waves and their contribution to ocean wave spectra. Part II: Observation," *J. Oceanogr.*, 51, 407–419, 1995.
- [8] B. J. Lipa and D. E. Barrick, "CODAR measurements of ocean surface parameters at ARSLOE – preliminary results," *IEEE Oceans 82 Conf. Rec.*, 901–906, 1982.

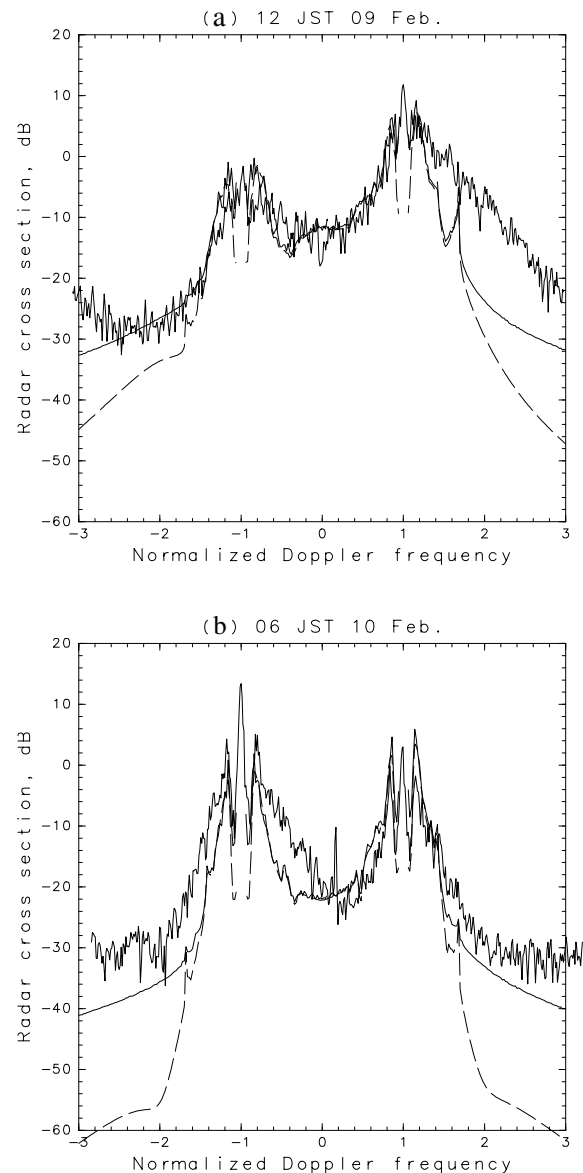


Fig. 7. Comparison of Doppler spectra. (a) 12 JST 9 Feb. 1998, significant waveheight=2.39 m. (b) 6 JST 10 Feb. 1998, significant waveheight=1.41 m. thin solid line :observed, thick solid line: predicted (finite illuminated area) thick dashed line: predicted (infinite illuminated area)